PART I

Phase Stability: Ion Bombardment and Solid State Reactions

SYNTHESIS OF BURIED SILICON COMPOUNDS USING ION IMPLANTATION

Alice E. White, K. T. Short, R. C. Dynes, J. M. Gibson, and R. Hull

AT&T Bell Laboratories
Murray Hill, NJ 07974

ABSTRACT

Ion implantation is widely used for doping semiconductors at low concentration, but, with the advent of a new generation of high current implanters, synthesizing new materials rather that simply doping them has become feasible. This technique has been successfully applied to fabricating silicon-on-insulator (SOI) structures with oxygen and nitrogen for several years. Since we are interested in understanding the mechanisms of formation of these layers, we have concentrated on sub-stoichiometric implantation doses of oxygen where it is easier to observe the coalescing layer. In order to determine whether this process of compound formation is more general, our studies were expanded to include implantation of the transition metals. Here, elevated substrate temperatures are necessary to minimize Si surface damage. The resulting disilicide layers are of remarkably high quality: they are single crystals in registry with the silicon wafer and they have better residual resistivities than comparable UHV-reacted silicides.

INTRODUCTION

Since ion implantation was invented almost 40 years ago, implanters have become permanent fixtures on integrated circuit processing lines. In fact, manufacture of today's chips can involve as many as 10 implantation steps. Implantation is used primarily at doses of 10^{12} - 10^{13} ions/cm^2 for doping the semiconductor to tailor the electrical properties. Other conventional uses of implantation include amorphization for isolation or fundamental solid state studies, mixing for phase formation, and heavy doping for contacts. In the past, applications of implantation were dominated by the small beam currents that were available, but recently a new generation of high current implanters has entered the market. It is this high current capability that allows us to implant the large concentrations required for compound formation--about five orders of magnitude higher than those required for doping.

In this paper, we will briefly discuss our results on the formation of substoichiometric buried oxide layers as the first example of compound synthesis in silicon. In order to determine whether this process was limited to SiO_2 and Si_3N_4, we decided to explore the silicides. Several of the silicides are very good conductors and, in general, they have high mechanical and thermal stability and are compatible with silicon processing. We started with $CoSi_2$ because of the demonstration of epitaxial growth of such films on silicon using Co deposition and reaction [1]. It has the CaF_2 structure and a small lattice mismatch with silicon, $\sim$1.2% at room temperature. Using this technique of

Mat. Res. Soc. Symp. Proc. Vol. 100. ©1988 Materials Research Society

implantation and annealing, we have grown buried single-crystal layers of $CoSi_2$ which are oriented with the silicon substrate. We call this technique mesotaxy, for arrangement *inside* the silicon. Structural and electrical results from the $CoSi_2$ layers as well as several other metal disilicides and a ternary silicide ($Co_{1-x}Ni_xSi_2$) will be presented.

FORMATION OF BURIED OXIDE LAYERS

For the last ten years, formation of buried oxide layers in silicon by ion implantation has been an active area of research for several groups investigating its viability as a silicon-on-insulator (SOI) technology [2]. Most of the previous work involved doses of oxygen of $\sim 2\times10^{18}/cm^2$, large enough to form a stoichiometric SiO_2 layer *during* the implant. When these are annealed at temperatures above 1200°C, the edges of the profile (which levels off when the stoichiometric concentration of oxygen is achieved) sharpen and the damage in the surface Si is partially removed. We decided, instead, to concentrate on sub-stoichiometric doses of oxygen where the peak concentration of implanted oxygen is below that required for SiO_2 (67 at. %). The advantages of using sub-stoichiometric doses are that lower doses mean shorter implantation times and fewer defects in the surface silicon. In addition, an SOI structure with thin SiO_2 layers has a higher capacitance and therefore requires lower charging voltages. Most importantly for us, however, is that it is easier to observe the process of formation in such layers without obscuration by a thick amorphous layer.

The basic process involves accelerating oxygen ions to hundreds of keVs and implanting them into a silicon wafer. Details of the thin buried oxide layer formation have been published elsewhere [3], but a brief review follows. At low substrate temperatures ($<\sim300$°C), a uniform, continuous buried oxide is formed at a depth of 4000Å with thickness $\sim$600Å after implantation of $3\times10^{17}O^+/cm^2$ at 200 keV and annealing at $\sim$1400°C for 1/2 hr. Although there is a 1500Å layer of crystalline silicon (10^8 defects/cm^2) on the surface, the buried oxide layer is bounded by twins which result from the imperfect regrowth of the heavily oxygenated silicon. The activation energy associated with the high temperature anneal has been shown to be $\sim$6eV, higher than the activation energy for forming SiO_2 and close to that for annealing silicon crystalline damage. We showed that the twins can be easily reduced by re-amorphization of the silicon overlayer followed by solid phase epitaxial growth at 600°C [3]. This is illustrated in Fig. 1. Implantation of a higher dose of oxygen ($\sim5\times10^{17}/cm^2$) at 1 MeV gives a layer which looks very similar, but is buried under almost 1μm of crystalline silicon.

If, however, the substrate temperature is raised above 400°C to anneal out more of the damage during implantation, very different behavior is observed. In this case, premature segregation of oxygen leads to a laminar structure of amorphous material imbedded in crystalline material in the region of the implant. When samples of this type are annealed at high temperatures, the growing oxide layer tends to isolate regions of silicon which cannot escape by diffusion. This was particularly easy to observe in our thin layers and results in uneven layers with a high density of silicon islands. These islands are also seen at the edges of thicker layers.

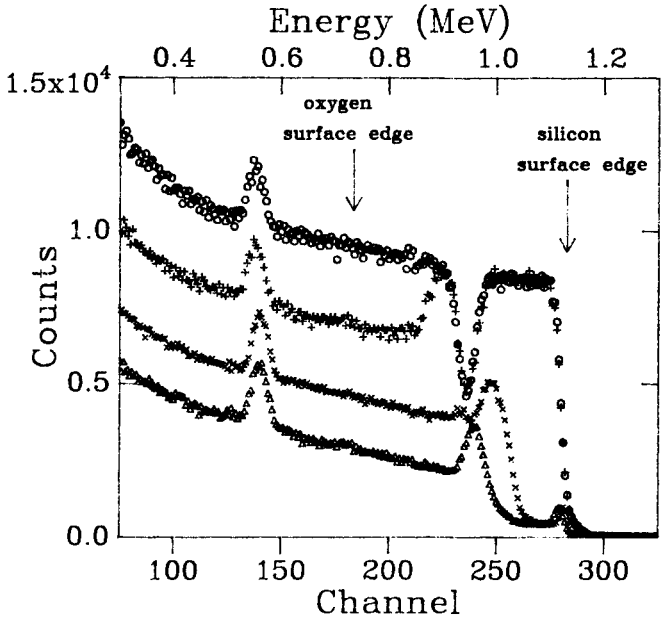

Fig. 1: RBS spectra for a thin buried oxide layer showing the decrease in the Si channeling yield in the region of the oxide layer due to re-amorphization and regrowth. Open circles are data from the random RBS spectrum of the annealed layer. Crosses show the channeled spectrum from the same sample after $3\times10^{14}Si^{+}/cm^{2}$ at 440 keV. After 1 hr. at 600°C, the channeling data is given by the open triangles. For comparison, the channeling data from the original layer are shown as X's.

We realized that what we were observing was a classic competition between nucleation and growth of SiO_2 precipitates where the kinetics are controlled by balancing the energetically favorable formation of new SiO_2 with the energetically unfavorable increases in surface tension. At low substrate temperatures, the implant damage leaves plenty of nucleation sites and homogeneous nucleation leads to formation of a uniform SiO_2 layer. However, twins appear because of poor regrowth of the silicon. At high substrate temperatures, dynamic annealing solves the twin problem, but premature growth of a limited number of SiO_2 precipitates results in nonuniform layers with silicon inclusions.

MESOTAXY: SYNTHESIS OF METAL DISILICIDES

The conventional process for growing silicides involves deposition of a metal film, usually in ultra-high vacuum (UHV), followed by reaction at ~600°C

to form the silicide. This results in extremely high quality epitaxial films with smooth interfaces on (111) Si, but the films are difficult to grow on (100) Si [1]. For mesotaxy, we start with implantation of 200 keV Co^+ ions to create a gaussian profile of Co atoms beneath the surface of a silicon wafer which is held at elevated temperature. When the sample is annealed 1000°C for 1/2 hr., the Co coalesces into a uniform buried single-crystal $CoSi_2$ layer with sharp interfaces in (111) and (100) Si [4]. A dose of $3\times10^{17} Co^+/cm^2$ gives an 1100Å thick layer--higher doses produce epitaxial surface layers and lower doses (above the threshold peak concentration mentioned below) result in thinner layers [5].

Rutherford Backscattering (RBS) and channeling studies of these films confirm that they are buried and aligned with the silicon substrate. The $CoSi_2$ layers have χ_{min}'s of 10-12% in (100) Si and as low as 6% in (111) Si, but these values are limited by the dechanneling in the defective surface Si. Additional dechanneling at the front and back edges of the $CoSi_2$ layer is evidence for the presence of interfacial defects. In the as-implanted sample, we observe up to 50% alignment in the Co portion of the spectra and attribute this to formation of oriented precipitates of $CoSi_2$ during the elevated temperature implant. The aligned fraction decreases with decreasing peak Co concentration. Annealing at 600°C for 1 hr. results in a slight sharpening of the profile and some improvement in axial alignment, but the transformation to a layer occurs only after a higher temperature anneal.

The incorporation of the Co into the buried silicide layer is amazingly complete as determined by secondary ion mass spectroscopy (SIMS). This is a difficult situation to study because the Si isotopes overlap ^{59}Co, but the results of a carefully calibrated measurement [6] are shown in Fig. 2. There we have plotted Co concentration on a logarithmic scale vs. depth (where the scale is approximated by measuring the depth of the milling hole). The Co concentration in the layer is close to that expected for $CoSi_2$, and the Co concentration in the surface and substrate Si is reduced by at least 5 orders of magnitude (the background level). This clearly illustrates the strength of the compound formation process.

The microstructural uniformity of the buried $CoSi_2$ layers is confirmed by transmission electron microscopy (TEM). Misfit dislocations in the silicide show that the layer is partially relaxed. Threading dislocations in the surface and loops in the substrate from annealing of the end of range damage are the major defects in the silicon. The quality of the interface is illustrated in Fig. 3 which is a direct lattice image of the top interface of a buried 900Å $CoSi_2$ layer in (100) Si. On a larger scale, a high density of defects at the interface (predicted from RBS) is apparent, but the (100) interfaces form with only a few small facets.

A. Threshold Peak Concentration

Reducing the dose yields a thinner silicide layer buried under a correspondingly thicker surface silicon layer, since the layers form at the depth of the peak concentration of implanted Co. For example, an implant dose of 1.6×10^{17} Co^+/cm^2 coalesces on annealing to a $CoSi_2$ layer which is ~600Å thick buried under 1100Å of silicon. However, when the dose is reduced by only 7% to $1.5\times10^{17}/cm^2$, annealing no longer produces a uniform layer. This apparent threshold is even more dramatic if the implant energy is reduced to

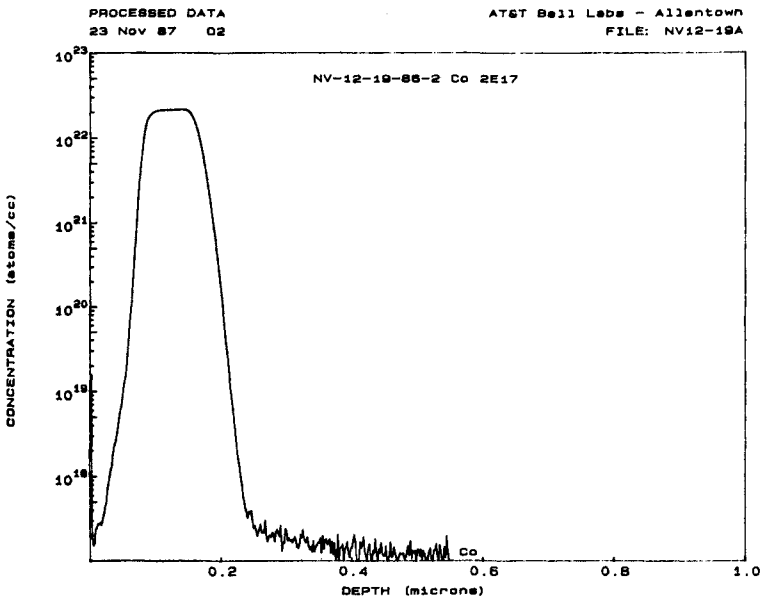

Fig. 2: SIMS spectrum [6] showing Co concentration vs. depth for a buried $CoSi_2$ layer formed by implantation of 2×10^{17} Co^+/cm^2 at 200 keV and 350°C into (100) Si and annealing at 600°C and 1000°C. Note how completely the Co has been incorporated in the layer.

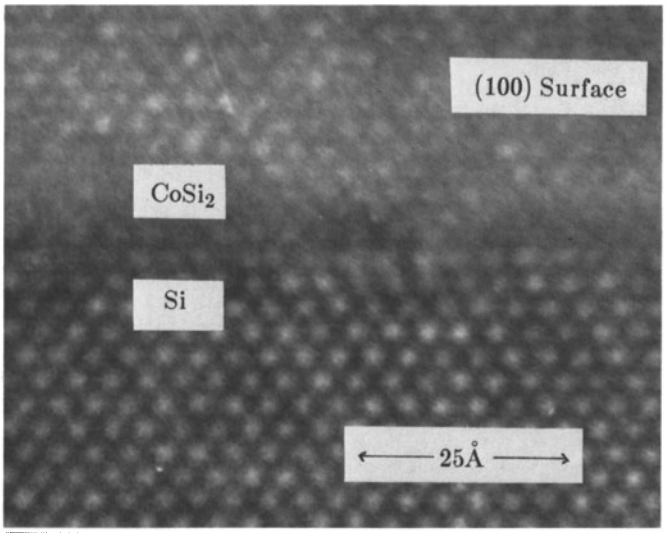

Fig. 3: HREM micrograph of the top $CoSi_2$/Si interface of a mesotaxy layer in (100) Si.

100 keV to reduce the spread in the implant profile. In this case, a dose of 1×10^{17} Co^+/cm^2 coalesces to a continuous layer <400Å thick. Again, however, a small reduction in dose to 0.9×10^{17} gives an implanted profile which fails to coalesce on annealing. This is seen in the random and channeled RBS spectra of the annealed samples (shown in Fig. 4). The random spectra from the as-implanted samples are overlaid for comparison. In Fig. 4a, the peak concentration increases markedly as the layer coalesces, but in Fig. 4b no change in the profile occurs on annealing (although the channeling yield does decrease). Although the minimum doses for layer formation at 100 keV and 200 keV differ by almost 50%, the peak implant concentrations (measured from the RBS spectra) are very similar for the two energies. These results indicate that *for these implant and annealing conditions,* the threshold concentration for layer formation is 18.5% +- 0.5 at. % of Co. This does not represent a lower bound, as we expect these numbers to be temperature-dependent.

When the two samples from Fig. 4 are examined in plan view TEM, the different morphologies are immediately descernible. Fig. 5a is the micrograph corresponding to Fig. 4a and it is indeed a continuous layer. The moire' fringes are due to interference from the different lattice spacings of the $CoSi_2$ and the underlying silicon. Below the threshold concentration (Fig. 5b, corresponding to Fig. 4b), we observe oriented $CoSi_2$ precipitates interspersed with Si "holes".

Many potential applications of this technique require lateral as well as vertical confinement of the layer. Although a focussed ion beam would be ideal here, we have demonstrated the feasibility of making fine lines by implanting through a 3000Å thick thermal SiO_2 mask. The pattern was a resolution test pattern with features as small as 1μm. The result is shown in Fig. 6 which is an SEM micrograph of a 1μm line (indicated by the arrow). Interestingly, there is actually a downward step in the Si in the region of the implant which is a function of dose and cannot be accounted for by the lattice contraction. The origins of this are not yet understood and we are studying it further. The bright debris on the wafer surface is just residual SiO_2 from an incomplete etching of the mask.

B. Electrical Results

We find that the structural integrity of these layers is reinforced by their electrical characteristics. If we plot the temperature dependence of the resistivity for several of these layers, the shape of the curves is similar to those published by Hensel et al. [7] for comparable UHV-reacted $CoSi_2$ layers (Fig. 7). This similarity in the shape of the curves implies that the temperature dependent phonon contribution to the resistivity is the same--i.e., they are basically the same material. However, the downward shift in the curves of the mesotaxy samples indicates that they have a lower residual resistivity.

We find that the best implanted silicide layers have residual resistivities which are almost a factor of two lower than the best UHV-grown $CoSi_2$ films and within a factor of two of the best bulk samples [4]. Possible explanations for these results are first that the improved residual resistivity results from the inherent cleanliness of the implantation process--the Co beam is mass-selected and therefore contains none of the common impurities present in Co evaporation sources and both of the interfaces are buried so the process is not surface sensitive. In addition, the buried films are more stable to high temperature anneals (surface films break apart at 1000°C). Finally, UHV-deposited films are thought to be slightly metal-rich [8]. Since ours are forming

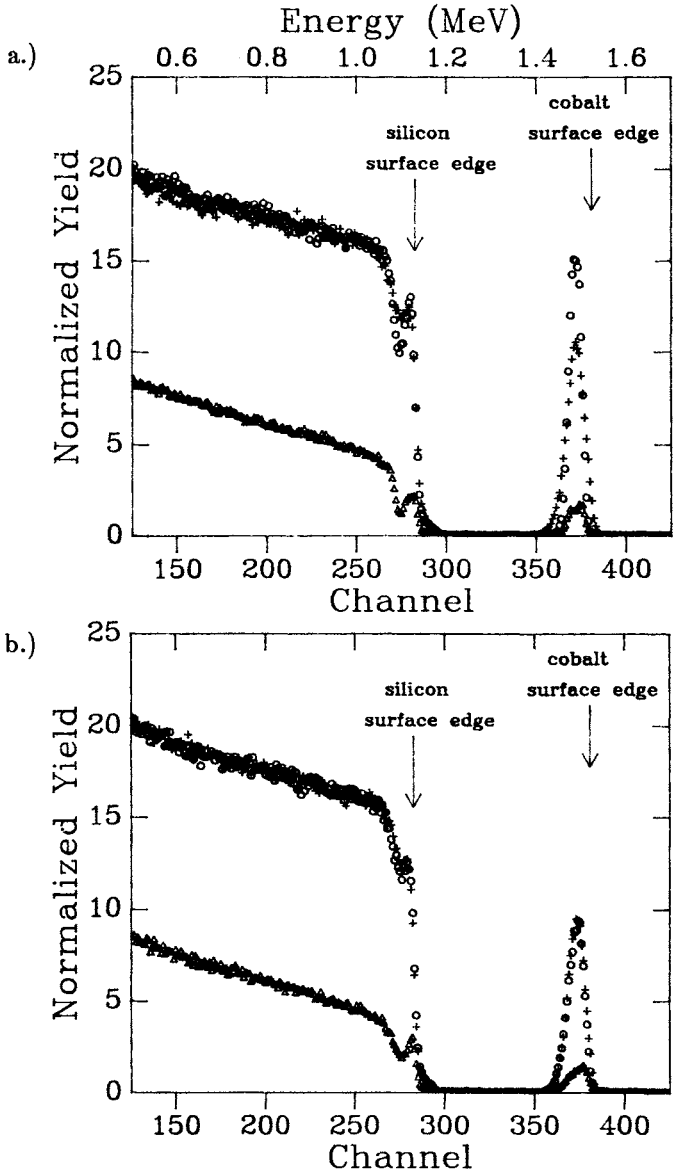

Fig 4: Random (circles) and aligned (triangles) RBS spectra (2 MeV He beam) for a.) a $1.0\times10^{17}Co^{+}/cm^{2}$ 100 keV implant b.) a sub-threshold $0.9\times10^{17}Co^{+}/cm^{2}$ 100 keV implant after annealing. The sample in a.) has coalesced to a complete layer while the sample in b.) has not. The random spectra from the respective as-implanted samples are superimposed (crosses) for comparison.

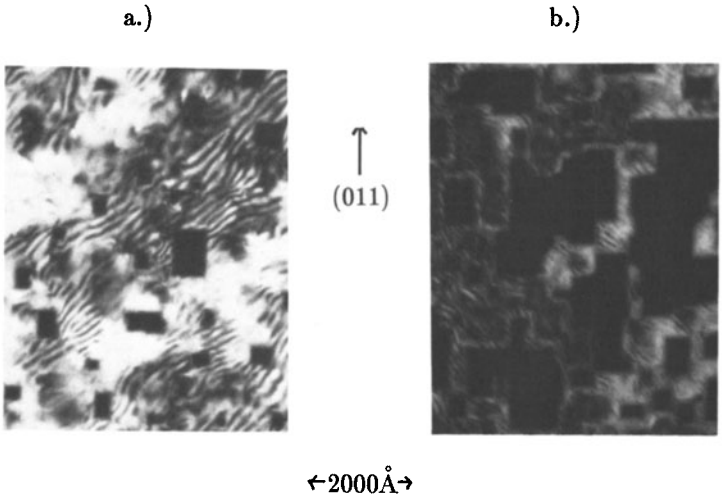

Fig. 5: Plan view TEM micrographs corresponding to the samples from Fig. 4a and 4b. These were imaged with the (200) reflection of $CoSi_2$, so the Si regions appear black.

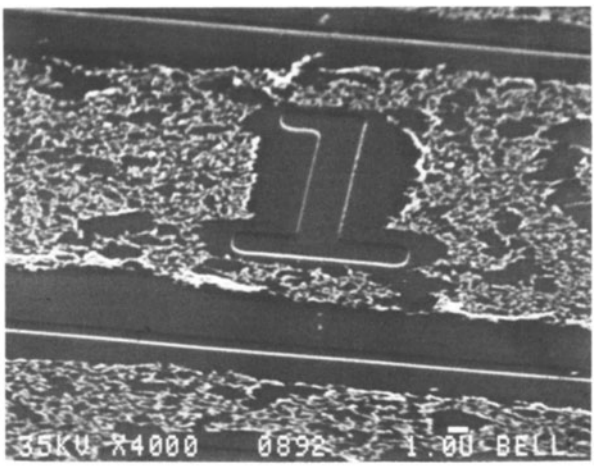

Fig. 6: SEM micrograph of a 1μm line of buried $CoSi_2$ created by implantation through an SiO_2 mask. The debris on the surface is just oxide left over from an incomplete etching of the mask.